E1 - Magnetic Pendulum – solution

Motivation

In the vibration isolation system of the VIRGO gravitational wave detector (see Fig. 1), repulsive magnets are used to shift the vertical oscillation frequency of the suspension from around 1.5 Hz to below 0.5 Hz. This improves the sensitivity of the detector to gravitational waves at a frequency of few Hz.

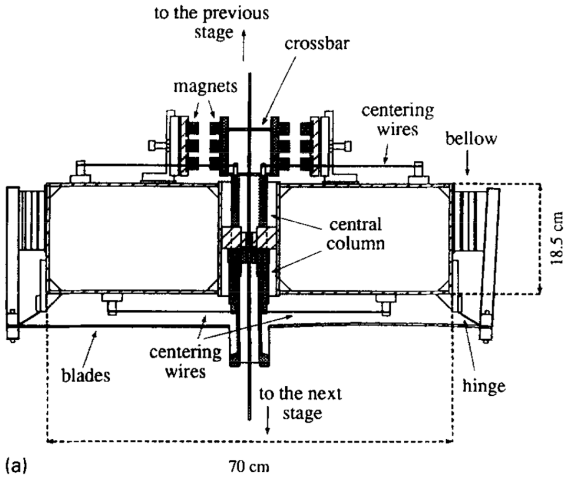

Figure 1: Magnetic anti-spring as part of the mechanical suspension of the VIRGO gravitational wave interferometer. From NIM A 394 (1997) 397-408.

Derivation of modified pendulum frequency (given to students)

The motion of a physical pendulum is constrained to the $y = 0$-plane (one degree of freedom). A magnetic dipole (oriented along the y-axis) is attached to the pendulum such that it is located at the origin when the pendulum is in equilibrium. Two more y-oriented magnetic dipoles are placed on the y-axis at $y = \pm d$. The combined dipole moment of the magnets on the pendulum is j_1, the dipole moments of the external magnets are both j_2.

The magnetic field at position $\vec{r}$ generated by a point dipole $\vec{m}$ at the origin, is:

$$\vec{B}(\vec{m},\vec{r}) = \frac{\mu_0}{4\pi}\cdot\left(\frac{3\vec{r}\cdot(\vec{m}\cdot\vec{r})}{r^5} - \frac{\vec{m}}{r^3}\right) \tag{1}$$

The y-component of the magnetic field generated on the x-axis by a dipole $(0, j_2, 0)$ located at $(0, d, 0)$ is therefore:

$$B_y(d,x) = \frac{\mu_0}{4\pi}\cdot j_2 \cdot \frac{2d^2 - x^2}{\left(x^2+d^2\right)^{5/2}} \tag{2}$$

The function is symmetric in d, so the two external magnets provide equal contributions on the x-axis. The first terms of a Taylor series around $x = 0$ are

$$B_y(d,x) = \frac{\mu_0}{4\pi}\cdot j_2 \cdot \left(\frac{2}{d^3} - \frac{6x^2}{d^5} + \frac{45}{4}\frac{x^4}{d^7} + \mathcal{O}\left(x^6\right)\right) \tag{3}$$

The potential energy of the pendulum as a function of its angle φ is:

$$U(\varphi) = Mgs(1-\cos\varphi) + j_1 \cdot 2B_y\left(d, 2\ell\cdot\sin(\varphi/2)\right), \tag{4}$$

where s is the distance from the magnetic pendulum COM to the pivot and ℓ is the distance from the pendulum magnet to the pivot. Neglecting constants and higher order terms:

$$U(\varphi) \approx Mgs\varphi^2/2 + \frac{\mu_0}{4\pi}\cdot j_1 \cdot 2j_2 \cdot \left(-\frac{6}{d^5}\ell^2\varphi^2\right), \tag{5}$$

$$U(\varphi) \approx \left(Mgs - \frac{6\mu_0}{\pi}\cdot j_1\cdot j_2\cdot\frac{\ell^2}{d^5}\right)\cdot\varphi^2/2, \tag{6}$$

The kinetic energy of the pendulum is $T(\dot\varphi) = I\dot\varphi^2/2$, from $\partial_\varphi U(\varphi) = \frac{\mathrm{d}}{\mathrm{d}t}\partial_{\dot\varphi}T(\dot\varphi)$ we find the natural frequency

$$\omega^2 = \left(Mgs - \frac{6\mu_0}{\pi}\cdot j_1\cdot j_2\cdot\frac{\ell^2}{d^5}\right)\Big/ I \tag{7}$$

We can write

$$\omega^2 = \omega_0^2 \pm \omega_{mag}^2 \tag{8}$$

with $\omega_0^2 = Mgs/I$ and $\omega_{mag}^2 = \frac{6\mu_0}{I\pi}\cdot j_1\cdot j_2\cdot\frac{\ell^2}{d^5}$, where the plus sign is for attractive external magnet polarity and the minus sign for repulsive external magnet polarity.

Task 1 - Mass of magnets and pendulum body (1.0 pts)

Without scales for weight measurements, there are multiple ways to determine the mass ratio between magnets and pendulum:

A) finding the center of mass of the pendulum with and without magnets (or with magnets in different positions)

B) finding the tilt angle of the pendulum with magnets offset horizontally (very precise by laser angle measurement)

C) measuring the pendulum frequency as a function of vertical magnet position, and using e.g. the position of fastest oscillation

The methods allow very different precision (with B best and C worst typically). Full score is achievable with any method if the numerical result is good.

All pendulums were weighed on an analytical balance. We measured a mass distribution for $M_{\text{pen}} = (44.7\pm1.7)$ g (mean and standard deviation). The mass of the two pendulum magnets agrees well with the specifications $M_{\text{mag}} = (7.68\pm0.01)$ g. The nominal mass ratio follows as

$$M/m = 5.82 \pm 0.22. \tag{9}$$

Measurements of twelve pendulum magnets are in agreement with the specified mass of 7.68 g for one pair. Separately measuring the six pairs reveals a sample standard deviation of only 0.035 g.

Table 1: Physical parameters of pendulum

quantity	value
mass of pendulum body	$M_{\text{pen}} = (44.7 \pm 1.7)\,\text{g}$
mass of pendulum magnets	$M_{\text{mag}} = (7.68 \pm 0.03)\,\text{g}$
distance magnets-axis	$\ell = (23.0 \pm 0.1)\,\text{cm}$
distance COM-axis (no magnets)	$s_0 = (12.0 \pm 0.1)\,\text{cm}$
distance COM-axis (with magnets)	$s_1 = (13.6 \pm 0.1)\,\text{cm}$
period without magnets	$T_0 = 2\pi/\omega_0 = (863 \pm 5)\,\text{ms}$
period with magnets	$T_1 = 2\pi/\omega_1 = (885 \pm 3)\,\text{ms}$
moment of inertia (with magnets)	$I = (1.38 \pm 0.02)\,\text{g}\cdot\text{m}^2$
dipole moment pendulum magnets	$j_1 = (0.96 \pm 0.01)\,\text{A}\cdot\text{m}^2$
dipole moment external magnet	$j_2 = (2.30 \pm 0.03)\,\text{A}\cdot\text{m}^2$

Since the magnet mass is more consistent between setups than the pendulum mass (and both measurements are fully anticorrelated by the given sum), points are awarded only for the determined magnet mass. The accepted range is chosen large enough to cover the spread in determined magnet mass caused by the variation in total mass relative to the given value of $52.3\,\text{g}$.

A: center of mass method By balancing the pendulum e.g. on a ruler, one can first mark the center of mass without magnets on the pendulum (S), then attach the magnets in a position P as far away from S as possible (e.g. bottom center), and measure the new center of mass (S'). Balance of torques around S' gives

$$M \cdot \overline{SS'} = m \cdot \overline{S'P} \tag{10}$$

With measured values of $\overline{SS'} = (1.6 \pm 0.1)\,\text{cm}$ and $\overline{S'P} = (9.4 \pm 0.1)\,\text{cm}$ one finds:

$$M/m = 5.9 \pm 0.4. \tag{11}$$

The separate masses can be expressed by the sum and ratio:

$$m = \frac{M+m}{1+M/m} = (7.6 \pm 0.5)\,\text{g} \tag{12}$$

$$M = (M+m) \cdot \frac{M/m}{1+M/m} = (44.7 \pm 0.6)\,\text{g}. \tag{13}$$

B: tilt angle method (lighter prototype pendulum) With the magnets placed at a position (x_m, y_m) relative to the pivot (projected onto the pendulum), the pendulum comes to rest at a tilt angle α relative to vertical. This angle can be measured precisely by observing the deflection δy of the laser spot at a screen distance d:

$$\tan\alpha = \delta y/d \tag{14}$$

N.B.: there is no factor two, since the rotation axis of the mirror is parallel to the laser beam.

Calling the angle between vertical and the line through pivot and magnet equilibrium position β, balance of torques becomes:

$$M \cdot s_0 \cdot \sin\alpha = m \cdot \sqrt{x_m^2 + y_m^2} \cdot \sin\beta \tag{15}$$

where

$$\tan(\alpha+\beta) = x_m/y_m \tag{16}$$

The COM distance from the pivot is $s_0 = (11.4 \pm 0.1)\,\text{cm}$. The best magnet position for a single measurement is close to the edge at the widest part of the pendulum. For $x_m = (7.7 \pm 0.1)\,\text{cm}$, $y_m = (18.0 \pm 0.1)\,\text{cm}$ and $d = (55 \pm 1)\,\text{cm}$, we obtained $\delta y = (5.9 \pm 0.1)\,\text{cm}$. From this we calculate $\alpha = 6.12°$, $\beta = 17.0°$, and $M/m = 4.7 \pm 0.4$.

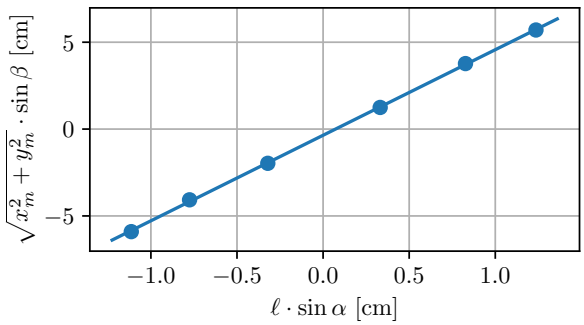

Figure 2: Analysis of tilt angle for several magnet positions.

For higher precision the balance of torques should be graphed for several magnet positions, see Fig. 2. The slope yields $M/m = 4.92 \pm 0.03$ (fit error only). The intercept of $(-0.36 \pm 0.02)\,\text{cm}$ can be explained by a failure to notice a 1 mm offset of the COM from the symmetry axis of the pendulum, rotating the coordinate system for β by $1°$.

C: frequency method (lighter prototype pendulum) The pendulum frequency depends on the position of the magnet placed at $(0, y)$ relative to the pivot as follows:

$$\omega^2 = \frac{Ms_0 + my}{I + my^2} \cdot g. \tag{17}$$

This function has a unique maximum ω_{max} at

$$y_{max} = \sqrt{I/M + \left(\frac{Ms_0}{m}\right)^2} - \frac{Ms_0}{m}. \tag{18}$$

Eliminating y_{max} from the expression for ω_{max}, we can solve for M/m:

$$m/M = \frac{4\omega_{max}^2}{\Omega^2} \cdot \left(\frac{\omega_{max}^2}{\omega_0^2} - 1 \right) \tag{19}$$

with $\Omega^2 = g/s_0$ and $\omega_1^2 = Ms_0g/I$.

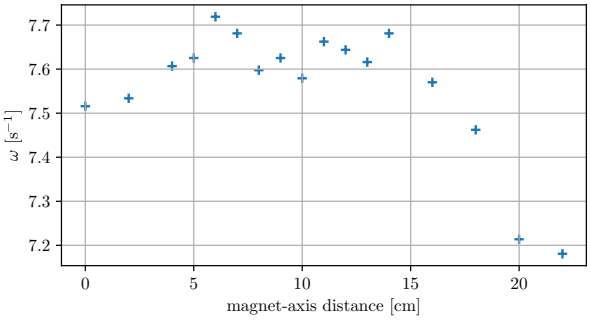

Figure 3: Pendulum frequency as a function of vertical magnet position.

After a scan of different y-values, we find $y_0 = (10 \pm 3)$ cm, $\omega_{max} = (7.65 \pm 0.05)\,\mathrm{s}^{-1}$, $\omega_1 = (7.50 \pm 0.06)\,\mathrm{s}^{-1}$ and $\Omega = (9.28 \pm 0.04)\,\mathrm{s}^{-1}$. We calculate $M/m = 6.7 \ldots 14$.

This method is not precise enough with the relatively high mass ratio of the setup.

variant: frequency with/without magnets There are many ways to extract the mass ratio from pendulum frequencies. A popular method was to compare the frequency with and without magnets, using only the nominal magnet position. The two expressions for the frequencies are

$$I \cdot \omega_0^2 = Mgs_0 \tag{20}$$

and

$$(I + m\ell^2) \cdot \omega_1^2 = (M + m)gs_1 \tag{21}$$

The mass ratio can be expressed as

$$M/m = \frac{\ell^2/g - s_1^2/\omega_1^2}{s_1^2/\omega_1^2 - s_0^2/\omega_0^2} = 6.1 \pm 0.3. \tag{22}$$

E1.1 – Masses		**Points**
A	**Center of mass method**	**0.6**
	Determination of distances $\overline{SS'}$ and $\overline{S'P}$ (0.1 per repetition with different magnet position)	0.4
	expression for mass ratio	0.2
B	**Tilt angle method**	**0.6**
	# of data points. 1:0.1, 2:0.3, ≥ 3: 0.4	0.4
	expression for mass ratio (or equivalent calculations for finding the masses)	0.2
C	**Frequency method**	**0.6**
	measurement of ω_1 and ω_0 (0.1 per repetition with $\geq$ 5 oscillations, or 0.1 per 10 oscillations without repetition)	0.4
	expression for mass ratio	0.2
	Numerical value for M_{mag}	**0.4**
	value inside (7.7 ± 1.0) g	or 0.2
	value inside (7.7 ± 1.5) g	or 0.1
	reasonable estimate of uncertainty	0.2
Total on Masses		**1.0**

Task 2 - Magnetic dipole moments (4.0 pts)

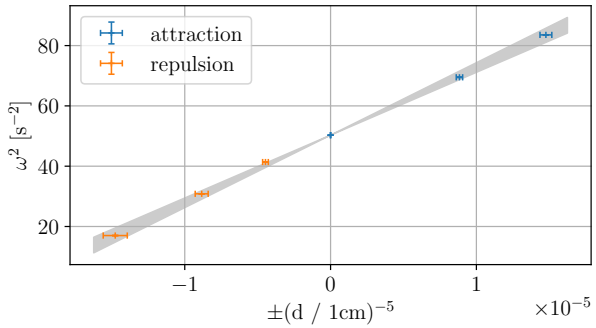

Figure 4: Determination of magnetic frequency shift by external dipole magnets.

a) Data collection The accessible frequency range is maximized by using both possible external dipole orientations. The closest possible distance in attractive orientation is given by stability of the magnets in the rail against sliding towards the pendulum, and is around $d = 7$ cm. In the repulsive mode it is given by the full compensation point near $d = 8.4$ cm, distances down to around 9 cm are practical.

For closer magnet spacings in repulsive mode, the pendulum moves in a double-well potential with an ill-defined behavior around zero amplitude. Eqn. **??** suggests a negative ω^2 and is not valid for oscillations around the off-set minimum. These data points are therefore not useful for this problem. This is specified in the hint that the magnets must be collinear when the pendulum is in equilibrium.

Since one needs to plot ω^2 vs d^{-5}, small d need to be sampled much more finely to spread the data points in d^{-5}. Ideally, one can pre-calculate an equal spacing, e.g. $(0^{-0.2}, 0.25^{-0.2}, 0.5^{-0.2}, 0.75^{-0.2}, 1^{-0.2}) \cdot d_0 =$

$(\infty, 1.32, 1.15, 1.06, 1) \cdot d_0$. The point at infinity is recorded by removing the magnets.

b) Specific magnetization Both attractive and repulsive datasets can be combined in one plot by counting repulsive magnet spacings as negative, absorbing the sign at $\pm\omega_{mag}^2$:

$$\omega^2 = \omega_1^2 + \frac{6\mu_0}{I\pi} \cdot j_1 \cdot j_2 \cdot \frac{\ell^2}{d^5} \tag{23}$$

Plotting ω^2 vs d^{-5}, one can fit a linear relation with slope $k = \frac{6\mu_0\ell^2}{I\pi} \cdot j_1 \cdot j_2$ and intercept ω_1^2.

The example data in Fig. 4 yield a slope of $k = (2.14 \pm 0.05)\,10^6\mathrm{cm}^5/\mathrm{s}^2$. To extract the dipole moment product one must measure the magnet-axis distance $\ell = (23.0 \pm 0.1)\,\mathrm{cm}$ and find the moment of inertia I. This can be extracted from the undisturbed frequency $\omega_1^2 = (M_{\mathrm{pend}} + M_{\mathrm{mag}})gs_1/I$, with the given total mass and gravitational acceleration, and the COM-axis distance $s_1 = (13.6 \pm 0.1)\,\mathrm{cm}$ (by balancing). One finds:

$$I = \frac{(M_{pend} + M_{mag})gs_1}{\omega_1^2} = (1.38 \pm 0.02)\,\mathrm{g \cdot m}^2 \tag{24}$$

The dipole moment product follows as

$$j_1 \cdot j_2 = k \cdot \frac{I\pi}{6\mu_0\ell^2} = (2.33 \pm 0.05)\,(\mathrm{Am}^2)^2. \tag{25}$$

Since the ratio $j_2/j_1 = 2.4$ is given, the dipole moments separately are

$$j_1 = \sqrt{j_1 \cdot j_2/2.4} = (0.98 \pm 0.01)\,\mathrm{Am}^2. \tag{26}$$

$$j_2 = \sqrt{j_1 \cdot j_2 \cdot 2.4} = (2.36 \pm 0.03)\,\mathrm{Am}^2. \tag{27}$$

With the true mass of the pendulum magnets $M_{magnets} = 7.68\,\mathrm{g}$ we find a specific magnetization of

$$j_1/M_{magnets} = (0.128 \pm 0.030)\,\mathrm{Am}^2/\mathrm{g}. \tag{28}$$

The expected value can be calculated from manufacturer values of remanence (1.29 T–1.32 T) and density ($7.4\,\mathrm{g/cm}^3$–$7.5\,\mathrm{g/cm}^3$) of NdFeB–N42:

$$\frac{B_r}{\mu_0 \cdot \rho} = 0.137\,\mathrm{Am}^2/\mathrm{g} - 0.142\,\mathrm{Am}^2/\mathrm{g}. \tag{29}$$

The 10% reduction of the observed specific magnetization may be explained by edge effects in the small magnets, where magnetization may not be homogeneous. There is a hint for edge effects also from the magnetic moment ratio between external and pendulum dipole moments, 2.4 measured with a magnetometer, higher than the volume ratio, 2.2 measured without the coatings.

The data collection and linear regression was performed for five different setups, the slope was consistent within ±5% (explained by observed magnetic moment variations) while the offset (squared frequencies) was stable within ±1%. The accepted numerical ranges cover this variation.

E1.2 – Magnetic Dipole Moments		**Points**
a)	**Frequency measurements**	**2.0**
	Both attraction and repulsion used	0.3
	Closest d setting $\leq 9\,\mathrm{cm}$ (0.1 if $\leq 10\,\mathrm{cm}$)	0.3
	Denser spacing for small $\lvert d\rvert$	0.3
	0.1 per different d-setting (incl. ∞)	0.6
	0.1 per 10 oscillations per d value	0.5
b)	**Specific magnetization**	**2.0**
	Graph of ω^2 vs d^{-5} or ω vs $d^{-5/2}$ or $\log\lvert\omega^2 - \omega_1^2\rvert$ vs $\log d$	(1.0)
	correctly enter data points (0.1 each)	0.5
	correct axis labels and ticks	0.1
	data covers $\geq \frac{1}{2}$ page	0.1
	trend line drawn	0.1
	slope read	0.1
	slope error estimated	0.1
	expression for determining I	0.3
	expression for determining $j_1 \cdot j_2$	0.2
	expression for determining j_1	0.2
	Numerical value for $j_1/M_{mag} = 0.125\,\mathrm{Am}^2/\mathrm{g}$, or alternatively $j_1 \cdot j_2 = 2.2\,(\mathrm{Am}^2)^2$ (0.3 within ±10%, 0.2 within ±20%, 0.1 within ±30%)	0.3
Total on Magnetic Dipole Moments		**4.0**

If, instead of a graphical analysis, a slope was calculated from two data points, we award 0.2/0.5 points for "entering data", no points for axis, space and trend line (total loss: 0.6 points). For the rest we apply the normal grading scheme.

Task 3 - Unknown external magnets (3.0 pts)

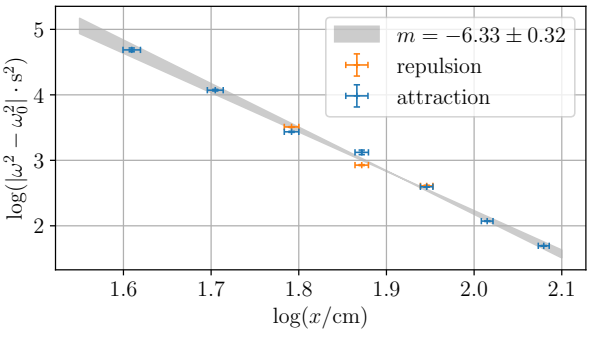

Figure 5: Determination of unknown magnet power law.

a) Data collection By experimentation one can find that the unknown magnets are symmetric under a 180° rotation, not anti-symmetric as the dipoles. It is still possible to obtain both attraction and repulsion, either by swapping the unknown magnets (which are given to be oppositely magnetized to each other), or by flipping the pendulum magnets. Flipping the pendulum magnets may require a new measurement of ω_1 if the magnet position is not exactly the same.

As the overall field strength is weaker, distances

down to $d = 5\,\text{cm}$ are possible in attractive mode, as well as about $d = 5.5\,\text{cm}$ in repulsive mode. For equal spacing in log-scale one can choose d values increasing by roughly the same factor between following measurements.

Attractive and repulsive mode can not be combined to increase precision, but can serve as independent measurements of the absolute value of magnetic frequency shift at a given separation. Only the attractive mode can be selected for its higher accessible d-range and overall faster frequencies (higher relative precision).

b) Power law Plotting the absolute value of the squared magnetic frequency shift $|\omega^2 - \omega_1^2|$ versus the magnet distance on double-logarithmic axes (Fig. 5), one can fit a linear relation with slope $a = -6.33 \pm 0.32$, indicating a power law $\omega_{mag}^2 \propto d^{-6}$.

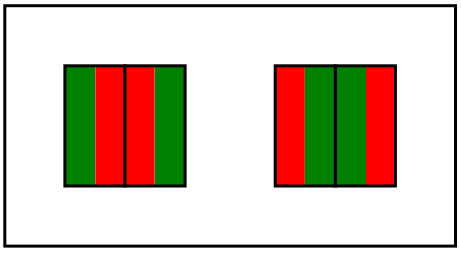

Figure 6: Dipole configuration of unknown external (quadrupole) magnets.

c) Dipole configuration Since the exponent of the magnetic frequency shift is one higher than for the dipole magnets, we can conclude that also the exponent of the magnetic field as a function of distance is one higher than for the dipole law, $B \propto r^{-4}$. (In fact the squared magnetic frequency shift follows the curvature of the magnetic field, the derivatives add two to the power law exponent.)

We are looking for a magnetic quadrupole configuration. This can be created by an arrangement of equal and opposite dipole magnets (canceling the total dipole moment of the arrangement). The simplest solution consistent with the package (see Fig. 6) consists of two coaxial and opposite cylindrical dipole magnets in each unknown external magnet, one with north poles facing out, one with south poles facing out.

Another valid solution is made of cylinders with radial magnetization (i.e. south poles towards the symmetry axis, north poles outwards, and vice versa). This would be harder to build but yields magnets indistinguishable from the actual ones to leading order.

Other possibilities of creating a quadrupole out of opposite dipoles (e.g. with dipole offset not parallel to the magnetic moments) are excluded because of the cylindrical symmetry of the unknown external magnets (this can be tested e.g. by rotation of the unknown magnet in a dipole field).

E1.3 - Unknown external magnets		**Points**
a)	**Data collection**	**1.0**
	Closest d setting $\leq 6\,\text{cm}$	0.2
	Denser spacing for small $\lvert d\rvert$	0.2
	0.1 per 2 different d-settings	0.3
	0.1 per 10 oscillations per d value	0.3
b)	**Power Law**	**1.5**
	Graph of $\ln\left(\lvert\omega^2 - \omega_1^2\rvert\right)$ vs $\ln(d)$	(1.0)
	correctly enter data points (0.1 each)	0.5
	correct axis labels and ticks	0.1
	data covers $\geq \frac{1}{2}$ page	0.1
	trend line drawn	0.1
	slope read	0.1
	slope error estimated	0.1
	Exponent value (-6 ± 0.5: 0.5, -6 ± 1: 0.2)	0.5
c)	**Dipole configuration**	**0.5**
	Sketch of possible dipole configuration	0.3
	justification (0.1 each for magnetic symmetry under reversal, locating the opposite pole in the center, magnetic cylindrical symmetry, or cancellation of dipole moments)	0.2
Total on Unknown external magnets		**3.0**

If, instead of a graphical analysis, a slope was calculated from two data points, we apply the grading scheme of 1.2b).

In 1.3c), if no points were awarded for justification, also no points are given for the correct configuration.

Task 4 - Nonlinear pendulum (2.0 pts)

a) Compensation Distance A precise way of finding the compensation distance is from the analysis of E1.2. We are interested in the x-intercept of the regression line, with slope $k = (2.14 \pm 0.05)\,10^6\text{cm}^5/\text{s}^2$ and y-intercept $\omega_1^2 = (50.3 \pm 0.3)\,\text{s}^{-2}$. We find $d_{comp}^5 = k/\omega_1^2$, or $d_{comp} = (8.43 \pm 0.05)\,\text{cm}$.

Another possibility is to manually approach the compensation point and carefully check for the absence of two separate minima.

A less useful method is the recording of the angular separation $\Delta\varphi$ of the split minima for $d < d_{comp}$ as a function of d. This relation is strongly curved and therefore not suited for a precise extrapolation to $\Delta\varphi = 0$.

b) Period Power Law Near the point of full compensation of the quadratic terms of gravitational and magnetic potential, an interesting dependence of pendulum frequency on amplitude can be observed.

Fig. 7 shows numerical calculations of the period for different magnet spacings close to full compensation (black) and without external magnets (red).

For experimentally achievable configurations, three ranges can be distinguished:

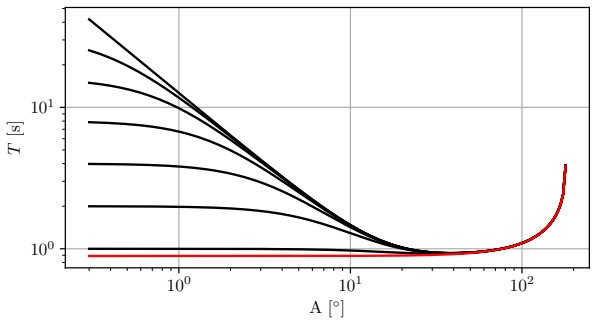

Figure 7: Numerical calculation of pendulum period versus amplitude, for different degrees of compensation.

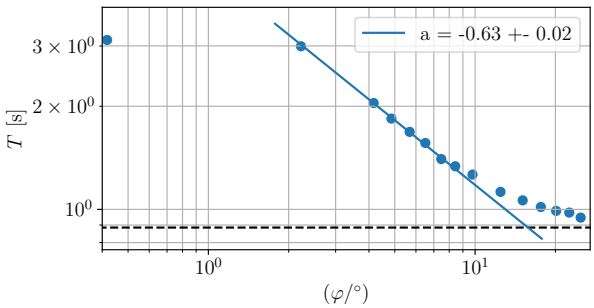

Figure 8: Measured pendulum period versus amplitude.

- for small amplitudes the period is constant, given by the small remaining quadratic potential term from imperfect compensation
- in an intermediate amplitude range, the magnetic quartic potential dominates, leading to a theoretical dependence $T(\varphi) \propto \varphi^{-1}$ with amplitude φ.
- for large amplitudes, the influence of the localized magnetic potential is small. The period approaches that of the undisturbed pendulum.

The extent of the relevant intermediate amplitude range depends on the quality of compensation, for example quantified by the ratio $T_0/T(\varphi = 0)$ of the compensated small-amplitude period to the small-amplitude period without magnets.

Typically the theoretical exponent of -1 is not reached in experiment, because the quartic potential does not fully dominate for any amplitude region. The expected maximum slope of the power law can be calculated numerically as a function of $T_0/T(\varphi = 0)$, see Fig. 9. (The exponent averaged over a factor of 2 in amplitude around the maximum is very close to this maximum value.)

The data shown in Fig. 8 was acquired with a compensation quality corresponding to $T_0/T(\varphi = 0) = 4.08$. This results in an expected maximum exponent of -0.645 (-0.63 when averaged over a factor 2 in amplitude). This agrees well with a linear regression around the steepest part of the amplitude-period relation.

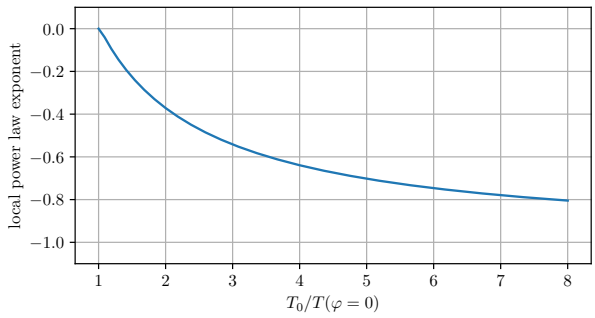

Figure 9: Maximum power law slope as a function of "degree of compensation".

E1.4 – Nonlinear Pendulum		**Points**
a)	**Cancellation point**	**0.5**
	Numerical value for $d_{comp} = (83.3 \pm 2.0)$ mm (0.2 within 4 mm)	0.5
b)	**Amplitude dependence**	**1.5**
	0.1 per 2 amplitude values	0.4
	0.1 per oscillation at each amplitude value	0.3
	double-logarithmic graph	0.5
	discussion (0.1 each for plateau at small amplitudes, power law at intermediate amplitudes, or plateau at large amplitudes)	0.3
Total on Nonlinear Pendulum		**2.0**

E2: Optical Black Box - Solution

Task E2.1 - Central element (∼0.3 pts)

To find out what element is located at the center of the box, we systematically beam into the box through all 4 ports (labeled A, B, C, D). We take note of where light exits. We deduce for the four options given:

- **no element**: Can be excluded because in that case we would only see light exiting from opposite ports but we can clearly see a signal around corners, e.g. exiting port B when beaming in through port A.
- **fully reflective mirror (both sides)**: This option we can also exclude since it would not allow for direct transmission along at least one of the optical axes. However, we can clearly see light passing from A to C and B to D (for some input polarizations).
- **regular-triangle-shaped prism:** A regular-triangle-shaped prism has a $60°$ angle between all surfaces. This configuration will always deflect a beam out of the optical axis, but as we clearly see that a central beam remains straight, the prism can be excluded.
- **semi-transparent mirror**: For every input beam, the box produces two significant output beams. This behaviour is well explained by a semi-transparent mirror. In fact we used a $2\,\mathrm{mm}$ thin acrylic glass plate with a semi-transparent window foil on one side.

To find out the orientation of the beam splitter (i.e. the orientation of the partially reflective surface), notice:

- To connect the two (perpendicular) optical axes of the black box, it needs to sit under a $45°$ angle with respect to both.
- Since ports A and B as well as C and D are connected, the partially reflective surface runs diagonally from the corner between D and A to the corner of B and C. (see Fig. 10)

E2.1 Central Element		Points
	Systematic observation of light splitting (automatically given if correct identification)	0.1
	Correct identification of semi-transparent mirror	0.1
	Correct deduction: Orientation of the mirror	0.1
Total on E2.1		**0.3**

Task E2.2 - Port elements (∼2.2 pts)

We systematically beam in through all four ports and write down the observed output for the remaining three ports. Also, we pay attention to effects resulting from a varying input polarization (by rotating the laser diode) and divergence and convergence of the beam. This way, we obtain the observation matrix Table 2.

From this, we conclude:

- **Polarizer at port D:** Whenever port D is involved, there is a strong polarization-dependent behavior and there is no polarization effect in all combinations not involving D. Therefore, D is a polarizer.
- **Diffraction Grating at port C:** There are always three beams coming out of port C. Therefore, there must be a diffraction grating at C. *Note: When beaming in through port C, the higher diffraction orders are clipped at the other ports such that there is only one beam exiting.*
- **Convex lens at port A:** Beaming along the axis connecting ports C-A, we can clearly see a focus outside the box - which can only come from the element at port A – and therefore, there must be a convex lens.
- **Concave lens at port B:** Along the axis B-D, we obtain a diverging beam. This could originate from a concave lens, or from a convex lens with a focus inside the box at B. The beam divergence is appar-

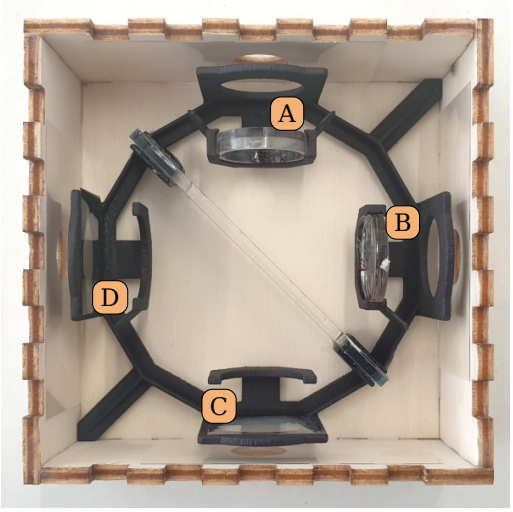

Figure 10: View inside the box

Table 2: Observed Light Properties when beaming in through one port (rows) and exiting through another (columns)

In ↓	Exit A	Exit B	Exit C	Exit D
A	-	focused beam, focus close to box	three focused beams, focus close to box	weak reflection, depends on input polarization
B	bright, focused beam, focus far away	-	three beams, very weak	diverging beam, depends on input polarization, intensity can be reduced to zero
C	focused beam, focus roughly 5cm away from box	very weak, diverging beam	-	collimated beam, depends on input polarization but intensity can not be reduced to zero
D	very weak, focused beam	diverging beam, depends on input polarization, intensity can almost be reduced to zero	three, collimated beams, depends on input polarization, intensity can almost be reduced to zero	-

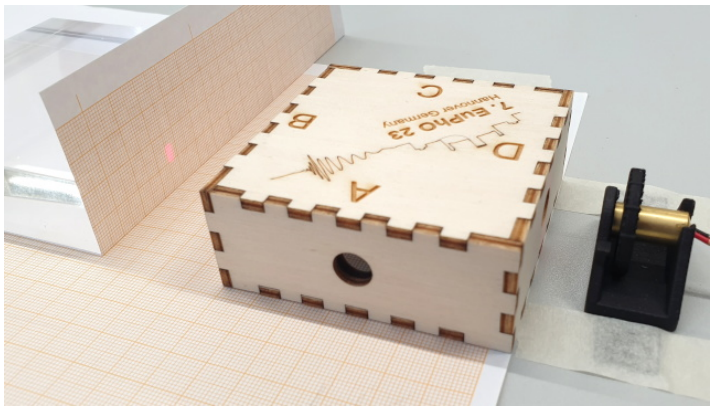

Figure 11: Setup to measure the diverging beam after the concave lens.

ently so flat that it does not converge to a focal spot within the area of B. Thus we conclude that at B, there is a concave lens.

E2.2 Elements		**Points**
a)	Recognizing or using the laser diode as a linearly polarized source of light	0.2
b)	**Observations and solution**	**2.0**
	A: observation / reasoning (beam focus)	0.2
	A: result focussing lens	0.3
	B: observation / reasoning (diverging beam)	0.2
	B: result concave lens	0.3
	C: observation / reasoning (separate spots)	0.2
	C: result grating	0.3
	D: observation / reasoning (rotation dependence)	0.2
	D: result polarizer	0.3
Total on E2.2		**2.2**

Task E2.3 - Properties (∼7.5 pts)

Now, we systematically conduct measurements to obtain the desired values of the four elements. Note that each window contains a protective glass plate of thickness $0.13\,\mathrm{mm}$, so the elements appear $0.04\,\mathrm{mm}$ closer to the box edge than they actually are. For true positions we use corrected values.

a) Convex lens behind port A (position and focal length) We start by verifying the beam exiting the laser being collimated with a constant spot size $w_0 \approx (3.8 \pm 0.2)\,\mathrm{mm}$ (may differ for each laser between $3\,\mathrm{mm}$ and $6\,\mathrm{mm}$). The possibility of a collimated beam is apparent from the Rayleigh range z_R (not required from students):

$$z_R = \frac{\pi w_0^2}{4\lambda} \approx 16\,\mathrm{m} \tag{30}$$

Realistically, the optical paths used in this setup will be below 50 cm, therefore, the widening of the Gaussian beam can be neglected in comparison to our measurement precision of the beam diameter.

Beaming in through port C (where we located the diffraction grating, whose zeroth order has the same beam profile as the incoming beam), we now measure the spot size as a function of distance from port A. We assign negative values to the spot diameters measured *after* the focus which we can roughly locate by eye to be at around 5 cm away from the box, to use a linear fit function for the beam envelope. The measured values are:

x [cm]	w [mm]
1	2.6
2	1.9
3	1.2
4	0.7
6	-1.0
7	-1.7
8	-2.1
9	-2.8
10	-3.2
11	-3.7
12	-4.3
13	-4.9
14	-5.3
15	-5.8

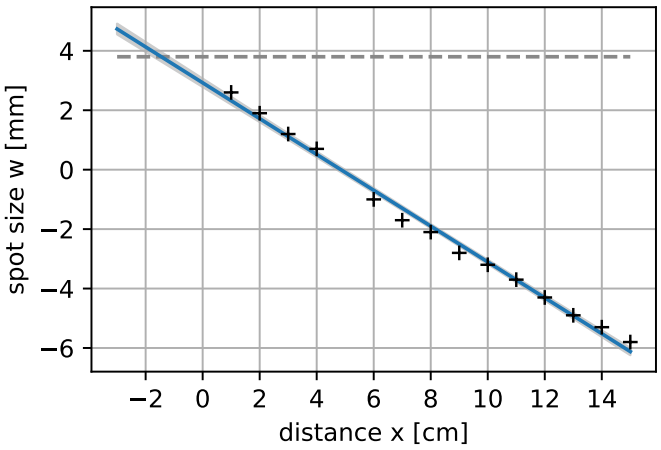

Figure 12: Linear fit of the spot size after the convex lens vs. distance from box edge

The spot size can therefore be described by a linear equation:

$$w(x) = w_0 - \frac{w_0}{f}(x - x_0) = -\frac{w_0}{f}x + w_0\left(\frac{x_0}{f} + 1\right). \tag{31}$$

Using the data plotted in Fig. 12, we obtain a focal length of

$$f = -\frac{w_0}{w_0/f} = \frac{3.8\,\mathrm{mm}}{0.0603} = (6.3 \pm 0.2)\,\mathrm{cm} \tag{32}$$

The true focal length is

$$f_{+,\mathrm{true}} = +6.5\,\mathrm{cm} \tag{33}$$

The position of the lens is found at the spot, where the converging beam diameter is equal to that of the

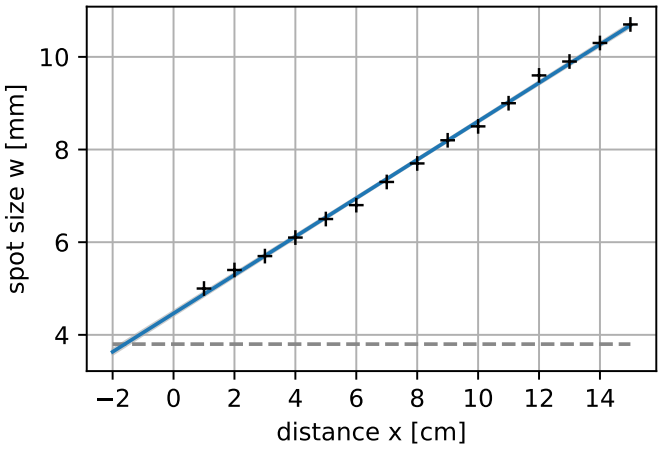

Figure 13: Linear fit of the spot size after the concave lens vs. distance from box edge

original collimated beam (cutting the dashed line in Fig. 12), which is $-1.7\,\mathrm{cm}$ from the edge at the box (while the edge is $3.8\,\mathrm{cm}$ from the center), thus

$$x_+ = 3.8\,\mathrm{cm} + x_0 = (2.1 \pm 0.3)\,\mathrm{cm} \tag{34}$$

The true position is

$$x_{+,\mathrm{true}} = 2.2\,\mathrm{cm} \tag{35}$$

from the center of the box.

b) Concave lens behind port B (position and focal length) To determine the position and focal length of the concave lens, we measure the size of the diverging beam at different positions. The position of the lens is located where the beam diameter would coincide with the original collimated beam.

We use the concave lens port B as an output, and insert the beam at port D, where the polarizer will not disturb the beam divergence. To measure the beam size at different positions, we tape a piece of paper with millimeter-scale onto the glass block, and mark the beam edges with a pencil. This allows us to measure the width with sub-mm precision (around $0.2\,\mathrm{mm}$ root-mean-squared).

The following recorded beam widths are shown in Fig. 13:

x [cm]	w [mm]
1	5.0
2	5.4
3	5.7
4	6.1
5	6.5
6	6.8
7	7.3
8	7.7
9	8.2
10	8.5
11	9.0
12	9.6
13	9.9
14	10.3
15	10.7

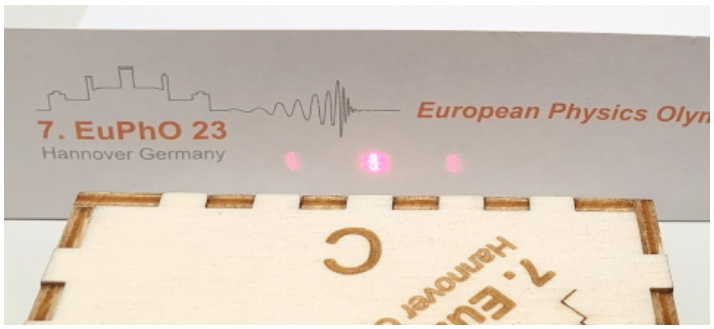

Figure 14: Setup for determining the grating distance and position.

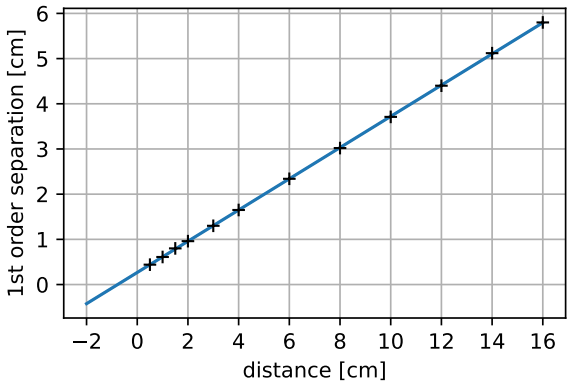

Figure 15: Linear fit of the first order separation over distance

From the fit, we determine the slope

$$w' = 0.0415 \pm 0.0005 \tag{36}$$

and the point $x_0 = (-1.6 \pm 0.1)\,\mathrm{cm}$, where the envelope cuts the original beam width $w_0 = 3.8\,\mathrm{mm}$

$$x_- = 3.8\,\mathrm{cm} + x_0 = (2.2 \pm 0.1)\,\mathrm{cm} \tag{37}$$

which is our estimate for the position of the concave lens. The true position is actually

$$x_{-,\mathrm{true}} = 2.1\,\mathrm{cm} \tag{38}$$

from the center of the box.

The focal length is determined by

$$f_- = -\frac{w_0}{w'} = (-9.2 \pm 0.3)\,\mathrm{cm} \tag{39}$$

The true focal length of the concave lens has been measured to be:

$$f_{-,\mathrm{true}} = (-9.2 \pm 0.15),\mathrm{cm} \tag{40}$$

Alternative method: For the measurement of the concave lens, it is also possible to move the box strictly sideways (e.g. along a fixed ruler) and measure the displacement of the beam at large distances. The possible displacement is around $7\,\mathrm{mm}$, and precisions around $5\,\%$ can be expected.

c) Diffraction grating behind port C (position, rotation and pitch) The grating produces two sharp side-beams of 1st and -1st order in horizontal direction. Therefore it is a linear grating with vertical lines (orientation). The line separation (pitch) can be determined by measuring the angle of the created beams relative to the 0th order transmission.

To avoid distraction from the lenses, we choose to enter through the polarizer (D) and exit through the grating at port C, and turn the laser to maximum transmission through the polarizer. By measuring the transversal beam separation at several distances from the box, we can fit the progression linearly, and obtain both the diverging angle and the offset position of the grating.

The diffraction angles α for each order n fulfill the relation

$$d \cdot \sin\alpha = n \cdot \lambda \tag{41}$$

where λ is the laser wavelength of $650\,\mathrm{nm}$.

We measured the following position values, where we have a higher point density near the box for a precise determination of the position, and a wide range of distances for a precise determination of the beam angle

x [cm]	y [cm]
0.5	0.44
1	0.61
1.5	0.80
2	0.96
3	1.3
4	1.65
6	2.34
8	3.02
10	3.71
12	4.4
14	5.12
16	5.8

which are plotted in Figure 15.

A linear fit yields the slope $y' = 0.3454 \pm 0.0005$ and a value of $y = 0$ at $x_0 = (-0.77 \pm 0.01)\,\mathrm{cm}$ and $\alpha = \arctan y' = 19.1°$. Therefore we determine the pitch as

$$d = \lambda / \sin\alpha = (1.99 \pm 0.02)\,\mu\mathrm{m} \tag{42}$$

The error of this is dominated by the uncertainty of the laser wavelength ($5\,\mathrm{nm}/650\,\mathrm{nm} = 0.8\,\%$), while the measured slope only has an uncertainty of $0.0005/0.3454 = 0.14\,\%$.

$$(\text{true value } 2\,\mu\mathrm{m}) \tag{43}$$

The position of the grating inside the box is where the fitted line cuts the x-axis. The main uncertainty for this stems from the placement accuracy of box and screen with roughly $1\,\mathrm{mm}$,

$$x_g = 3.8\,\mathrm{cm} + x_0 = (3.0 \pm 0.1)\,\mathrm{cm} \tag{44}$$

from the outer edge of the box. The true value is $x_{g,\mathrm{true}} = 3.12\,\mathrm{cm}$.

Figure 16: Determination of the laser polarization using Brewster reflection. The reflected beam will vanish at horizontal polarization.

d) Polarizer behind port D (rotation angle) To characterize the polarizer, we need to know the precise polarization of the laser beam. The laser can be characterized with the available acrylic glass block, using reflection from the surface under an angle. In particular, there is the Brewster angle, at which the incident light will be fully separated into two orthogonally polarized components. This Brewster angle can be computed from the given optical density, but more easily it can be probed by minimizing the intensity of a reflected beam.

The students may set the incident angle on a vertical glass surface to the Brewster angle, and simultaneously turn the laser around its optical axis to yield zero reflection (Fig. 16). This is the point where the laser is purely horizontally polarized, and may be marked on the turning wheel.

Now, to probe the polarizer, the laser is sent into the polarizer port (D) as an input. It should not be used as an output, because the central beam splitter might be partially polarizing and thereby disturb the measurement.

Subsequently, the angle of the polarizer is found by turning the laser around its optical axis until the transmission is minimized near zero (The minimum can be found more precisely than the maximum, because the relative intensity change remains large). This angle is noted relative to the angle of vertical laser polarization, and marks the direction of maximum suppression. Thus, the transmitting direction of the polarizer is $90°$ from the measured angle.

The polarization angle is found to be $65°$ from the vertical axis. we do not consider the orientation with respect to mirroring, only the angle from the horizontal axis.

As the measurement of the point of minimal transmission is quick, but not very precise, a good strategy is to take two measurements $180°$ apart and average their results.

E2.3 Properties		**Points**
a)	**Convex lens at A**	**1.9**
	Measurement idea and linearization: beam diameter as function of distance	0.2
	Data collection, at least 10 data points over 15 cm, in case of less: min(0.05 pts × number of measurements, s [cm]/30 pts for data range s, 0.5 pts total). (Alternatively located the focal spot quantitatively: 0.2 pts)	0.5
	Diagram and fit, alternatively analytic	0.6
	Result for $f = 6.5$ cm (± 0.5 cm, half for ± 2 cm)	0.2
	Result for $x_+ = 2.2$ cm (± 0.3 cm, half for ± 0.6 cm)	0.2
	Error propagation and estimation	0.2
b)	**Concave lens at B**	**1.9**
	Measurement idea and linearization: beam diameter as function of distance	0.2
	Data collection, at least 10 data points over 15 cm, in case of less: min(0.05 pts × number of measurements, s [cm]/30 pts for data range s, 0.5 pts total).	0.5
	Diagram and fit, alternatively analytic	0.6
	Result for $f = -9.2$ cm (± 1 cm, half for ± 2 cm)	0.2
	Result for $x_- = 2.2$ cm (± 0.3 cm, half for ± 0.6 cm)	0.2
	Error propagation and estimation	0.2
c)	**Diffraction grating at C**	**1.9**
	Correct pattern orientation (vertical lines)	0.2
	Measurement idea and linearization: diffraction order separation as function of distance	0.2
	Data collection, at least 3 data points over 15 cm. In case of less: min(0.2 pts × number of measurements, s [cm]/30 pts for data range s, 0.5 pts total).	0.5
	Diagram and fit, alternatively analytic	0.4
	Result for $d = 2\,\mu$m ($\pm 0.05\,\mu$m, half for $\pm 0.1\,\mu$m)	0.2
	Result for $x_g = 3.12$ cm (± 0.2 cm, half for ± 0.4 cm)	0.2
	Error propagation and estimation	0.2
d)	**Polarizer at D**	**1.8**
	Use Brewster angle configuration to determine laser polarization (0.1 for idea to use reflections from a dielectric to investigate polarization)	0.4
	When reflected beam intensity is (close to) zero, then horizontally polarized	0.2
	Noticing that the behavior is different when D is used as an out- vs. input.	0.2
	Use port D as input, not as output (and mention that)	0.2
	Use min, not max transmission	0.2
	Result $\lvert\alpha\rvert = 65°$ 0.3pts for $\pm 5°$ (0.2pts for $\pm 9°$) and 0.1pts for orientation closer to horizontal axis. (0pts if there was no plausible way to calibrate the polarization)	0.4
	Error estimation	0.2
Total on E2.2		**7.5**